ELECTRON AND HOLE g FACTOR ANISOTROPY IN CdTe/CdMgTe QUANTUM WELLS

A. A. Kiselev[1], E.L. Ivchenko[1], A.A. Sirenko[1,2], T. Ruf[2], M. Cardona[2], D.R. Yakovlev[1,3], W. Ossau[3], A. Waag[3], and G. Landwehr[3]

[1] *A.F. Ioffe Physico-Technical Institute, 194021 St. Petersburg, Russia*

[2] *Max-Planck-Institut für Festkörperforschung, 70569 Stuttgart, Germany*

[3] *Physikalisches Institut der Universität Würzburg, 97074 Würzburg, Germany*

Abstract

Effective g factors of electrons and heavy holes in CdTe/CdMgTe quantum wells have been measured with high accuracy as a function of the angle between the magnetic field and the structure growth axis. As a result, we have observed the electron g factor anisotropy in A_2B_6-based heterostructures. The dependencies of the g factor tensor components on the quantum well width and the solid solution composition have been calculated within the $\boldsymbol{k} \cdot \boldsymbol{p}$ method and compared with the available experimental data.

Keywords: semiconductors, quantum wells, electronic band structure, spin-orbit effects, spin-flip Raman scattering.

PACS: 71.18.+y, 71.20.-b, 73.20.Dx, 78.30.-j

A precise knowledge of g factors is important for the interpretation of magneto-optics, magneto-transport, resonant spectroscopy on spin-split sublevels, and light scattering experiments. Various experimental techniques have been applied to study exciton and free-carrier g factors in semiconductor heterostructures (see Ref. [1] and references therein). Nevertheless, the experimental data base for electron and hole g factors in low-dimensional systems is far from being complete and limited predominantly to the A_3B_5 heterostructures. Only very recently g factors in narrow (20–100 Å) and wide (80–300 Å) CdTe/CdMgTe quantum wells (QWs) have been measured by means of resonant spin-flip Raman scattering (SFRS) [1] and quantum-beat spectroscopy and photoluminescence (PL) [2], respectively.

In this paper we focus on the comparison of calculations of the electron and hole g factors with experimental data obtained by SFRS, which has been proven to be one of the most reliable experimental techniques for the direct determination of g factors in low-dimensional systems. The components of the g factor tensor are calculated in the framework of the $\boldsymbol{k \cdot p}$ theory for both electrons and holes as a function of layer width and solid solution composition. Effects of the strain (induced by the lattice-constant mismatch) on the g factor values are analysed and compared to the size-confinement effects.

CdTe/CdMgTe heterostructures with type-I band alignment were grown by molecular-beam epitaxy on (001)-oriented CdTe and $Cd_{0.97}Zn_{0.03}Te$ substrates. CdTe single QWs with widths between 18 and 100 Å are sandwiched between $Cd_{1-x}Mg_xTe$ barriers with $x = 0.15$, 0.26 and 0.5. Further information about the sample parameters, their characterization and the experimental setup has been published elsewhere [1].

In a magnetic field we observe two narrow Stokes (and anti-Stokes) SFRS lines for excitation in resonance with the heavy-hole exciton transition. These lines are attributed to exciton and electron spin-flip processes. The spin-flip shifts of the electron and exciton lines, Δ_{ex} and Δ_e, are proportional to the magnetic field, B. Since the exchange splittings of the exciton levels at $B = 0$ are small compared to the observed Zeeman splittings and can be disregarded hereafter, Δ_{ex} and Δ_e are proportional to the exciton and electron g factors (see Ref. [1] for discussion about the g factor signs). The heavy-hole g factor is determined by the relation $g^{hh} = g^{ex} + g^e$. In the magnetic field making an angle φ with the QW growth

axis,

$$|g^{e,h}(\varphi)| = \sqrt{(g_{\|}^{e,h}\cos\varphi)^2 + (g_{\perp}^{e,h}\sin\varphi)^2}.$$

The g factor components were obtained from the fit of this equation to the experimental angle dependences.

Values of both electron g factor components for a series of single QW structures $CdTe/Cd_{1-x}Mg_xTe$ with $x = 0.15$ are shown in Fig. 1 by solid ($g_{\|}$) and open ($g_{\perp}$) squares. We have also included in this graph the results of Ref. [2] (circles, $x = 0.25$) which considerably extends the range of QW widths available for the comparison with theory. Note that the quantum-beat technique applied in Ref. [2] only allows one to measure the transverse g factor, $g_{\perp}$.

In order to calculate the electron g factor we apply the Kane model. Thus, the $k_z p_z$ mixing between $|\frac{c}{6}\rangle$, $|\frac{v}{8}\rangle$ and $|\frac{v}{7}\rangle$ is taken into account exactly. The $k_x p_x$ and $k_y p_y$ terms are treated by second-order perturbation theory, which is sufficient for the g factor calculation [3]. For the conduction subband $e1$, the g factor components are given by [3]

$$g_{\|} = g_0 f_{\|} + \frac{1}{m_0}\sum_n (|\langle e1,1/2|p_+|n\rangle|^2 - |\langle e1,1/2|p_-|n\rangle|^2)\frac{1}{E_{e1}^0 - E_n^0},$$
$$g_{\perp} = g_0 f_{\perp} - \frac{2}{m_0}\sum_n \mathrm{Re}(\langle e1,1/2|p_+|n\rangle\langle n|p_z|e1,-1/2\rangle)\frac{1}{E_{e1}^0 - E_n^0}. \qquad (1)$$

Here m_0, g_0 are the free-electron mass and Lande factor, $p_{\pm} = p_x \pm i p_y$, $\langle n|p_\alpha|m\rangle$ ($\alpha = x, y, z$) is the momentum operator matrix element taken, in a single-QW structure, between the subband states n, m at the extremum $k_x = k_y = 0$ and, in a superlattice, between the miniband states n, m at $k_x = k_y = Q = 0$, where Q is the wave vector component describing the electron motion along z. E_n^0 is the electron energy at this point. The coefficients $f_{\|}$, $f_{\perp}$ are close to unity and take into account that the average spin component for an electron in the state $|e1, \pm 1/2\rangle$ differs slightly from $\pm 1/2$ even at the extremum because of the $k_z p_z$-induced mixing with valence band states.

The lattice mismatch between zinc-blende MgTe and CdTe is 1.0%. Shifts of the CdTe conduction and valence band edges due to the strain are included in the calculation procedure. We assume the barrier material to be unstrained which is valid in the case of thick barrier layers. Thus, the heavy- and light-hole states in the CdTe/CdMgTe QWs are split

due to both confinement and stress caused by the lattice mismatch between the compositional materials. In the CdTe/CdMgTe heterosystem, these two effects act in the same direction and push the light-hole states towards higher energies.

The solid (dotted) lines in Fig. 1 show calculated dependences of $g_{\parallel}^{e}$ and $g_{\perp}^{e}$ on the well width for CdTe/$Cd_{1-x}Mg_xTe$ QW with $x = 0.15$ (0.26). A small fixed contribution of remote bands has been added to Eqs. (1). This allows to get in the calculations (neglecting the strain) values of $g_{\parallel}^{e}$ and $g_{\perp}^{e}$ which in the limit of very thick QWs are close to -1.64 (g factor in bulk CdTe) and, at the same time, for ultra-thin QWs tend to -0.80 (g factor in bulk $Cd_{0.85}Mg_{0.15}Te$). One can see from Fig. 1 that the theory is in a rather good agreement with experiment despite the absence of other fitting parameters.

The experimentally measured electron g factor anisotropy, $(g_{\perp}^{e} - g_{\parallel}^{e})$, as a function of the QW width is presented by squares in the inset of Fig. 1. The reduction of the system symmetry due to uniaxial strain and spatial confinement leads to the g factor anisotropy as well as to the splitting of the , $^{v}_{8}$ band into the light- and heavy-hole subbands. The g-factor anisotropy exhibits non-monotonic behavior and, for CdTe/$Cd_{0.85}Mg_{0.15}Te$ QW structures, reaches a maximum for well widths $\sim$ 40 Å. The quantum-confinement-induced part of the g factor anisotropy is presented by the dashed curve. In quantum wells thinner than 80 Å the two contributions are found to be comparable in magnitude. In wider wells the strain-induced contribution dominates.

The electron g factor anisotropy is a continuous function of the QW width and vanishes for widths very large or close to zero. In contrast, the strong heavy-hole g factor anisotropy, $|g_{\perp}^{h}| \ll |g_{\parallel}^{h}|$, appears as soon as the degeneracy between the heavy- and light-hole states is lifted. The measured angle dependence of the heavy-hole g factor confirms that the value of $g_{\perp}^{h}$ is close to zero. For the samples with $x = 0.15$, the longitudinal component is shown in Fig. 2 as a function of the well width (squares). The sum $(g_{\parallel}^{ex} + g_{\perp}^{e})$ found from Ref. [2] is presented by circles. It can serve as a good estimate of $g_{\parallel}^{h}$. The uncertainty connected with the electron g factor anisotropy lies within the accuracy of the exciton g factor determination from the Zeeman splittings of the exciton transitions in PL and transmission experiments [2].

The simple Kane model which exactly takes into account the $\boldsymbol{k} \cdot \boldsymbol{p}$ interaction of the

, $_6^c$, , $_8^v$, and , $_7^v$ bands is insufficient for calculations of heavy-hole properties. In particular, it yields a negative heavy-hole effective mass $m_{hh} = -m_0$. As is well-known, a positive value of m_{hh} arises due to the $\boldsymbol{k} \cdot \boldsymbol{p}$ contribution of the remote conduction bands , $_8^c$ + , $_7^c$. We use in the heavy-hole g factor calculations the complete 8×8 $\boldsymbol{k} \cdot \boldsymbol{p}$ Hamiltonian which has advantages compared to the Kane model since it describes completely the coupling between the , $_6^c$, , $_8^v$, and , $_7^v$ bands and includes the contributions of the remote bands in an approximation the quadratic in $\boldsymbol{k}$ [4].

The solid (dotted) line in Fig. 2 shows a calculation of $g_{\|}^h$ for $x = 0.15$ (0.26). Since the band parameters for A_2B_6 semiconductors are known to a much less extent than those for A_3B_5 compounds, a simple fitting procedure has been carried out to find the Luttinger parameters for CdTe. Using the the spherical approximation ($\gamma_2^L = \gamma_3^L$) and neglecting contributions of remote bands with , $_4$ symmetry, one finds

$$\kappa^L = \frac{1}{3}(2\gamma_2^L + 3\gamma_3^L - \gamma_1^L - 2).$$

We applied this procedure to the set of experimental data for the samples with $x = 0.15$ and obtained the following Luttinger parameters: $\gamma_1^L = 5.1$, $\gamma_2^L \equiv \gamma_3^L = 1.66$, $\kappa^L = 0.4$. In Fig. 2 the dotted line ($x = 0.26$) is plotted with the same set of γ_i^L, κ^L.

In summary, by resonant SFRS we have measured with high accuracy the electron, exciton and heavy-hole g factors in CdTe/CdMgTe QWs. We developed a theory which takes the complicated valence-band structure as well as quantum-confinement and strain-induced effects into account. It provides a consistent description of the observed g factors as a function of the QW width.

Acknowledgements — This work has been supported in part by INTAS (grant 93-3657-Ext) and the Deutsche Forschungsgemeinschaft through SFB 410. A.A. Sirenko would like thank the Alexander von Humboldt Foundation for financial support.

REFERENCES

[1] A.A. Sirenko, T. Ruf, M. Cardona, D.R. Yakovlev, W. Ossau, A. Waag, and G. Landwehr, Phys. Rev. B **56**, 2114 (1997).

[2] Q.X. Zhao, M. Oestreich, and N. Magnea, Appl. Phys. Lett. **69**, 3704 (1996).

[3] E.L. Ivchenko and A.A. Kiselev, Fiz. Tekh. Poluprovodn. **26**, 1471 (1992) [Sov. Phys. Semicond. **26**, 827 (1992)].

[4] A.A. Kiselev and L.V. Moiseev, Fiz. Tverd. Tela **38**, (1996) 1574 [Phys. Solid State **38**, 866 (1996)].

FIGURES

FIG. 1. The well-width dependence of the electron g factor at the bottom of the first subband in CdTe/$Cd_{1-x}Mg_xTe$ single QWs. Full and empty squares show the SFRS data on longitudinal, $g_{||} \equiv g_{zz}$, and transverse, $g_{\perp} \equiv g_{xx} = g_{yy}$, components, respectively, measured in the structure with a Mg content $x = 0.15$. Circles show the data of Ref. [2] ($g_{\perp}$ component only, $x = 0.25$). Results of the Kane-model calculations are presented by solid ($x = 0.15$) and dotted ($x = 0.26$) lines. The inset shows the g factor anisotropy, $(g_{\perp} - g_{||})$, for the sample with $x = 0.15$: squares, experiment; full line, calculations; dashed, calculations representing only the quantum-confinement-induced contribution to $(g_{\perp} - g_{||})$.

FIG. 2. The heavy-hole longitudinal g factor, $g^h_{||}$, as a function of the QW width. Squares, SFRS data for $x = 0.15$; circles, combined quantum-beat / luminescence measurements for $x = 0.25$ [2]; solid and dotted lines, calculations for $x = 0.15$ and $x = 0.26$, respectively.

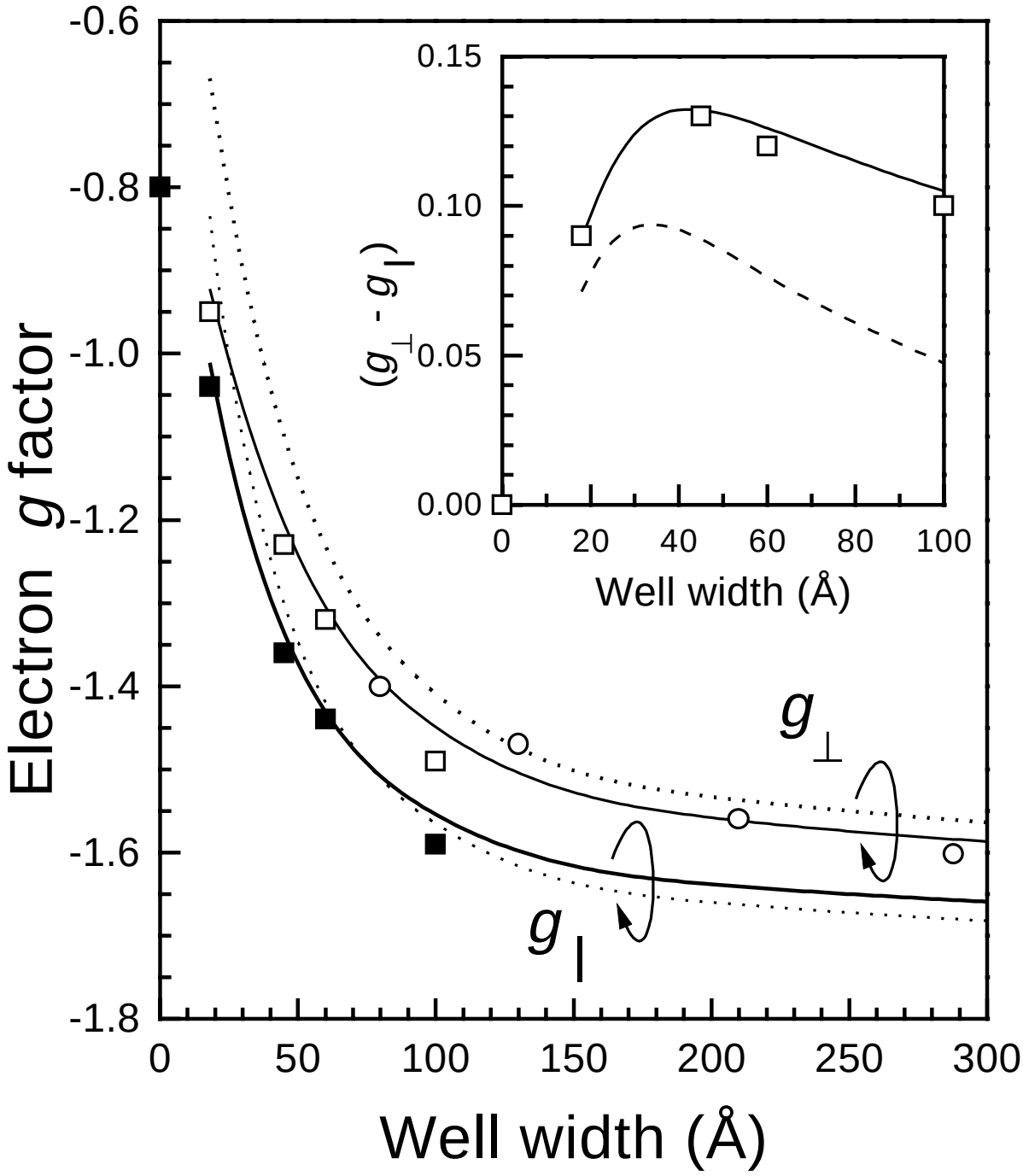

Fig. 1. Kiselev et al., A2B6 Conference in Grenoble

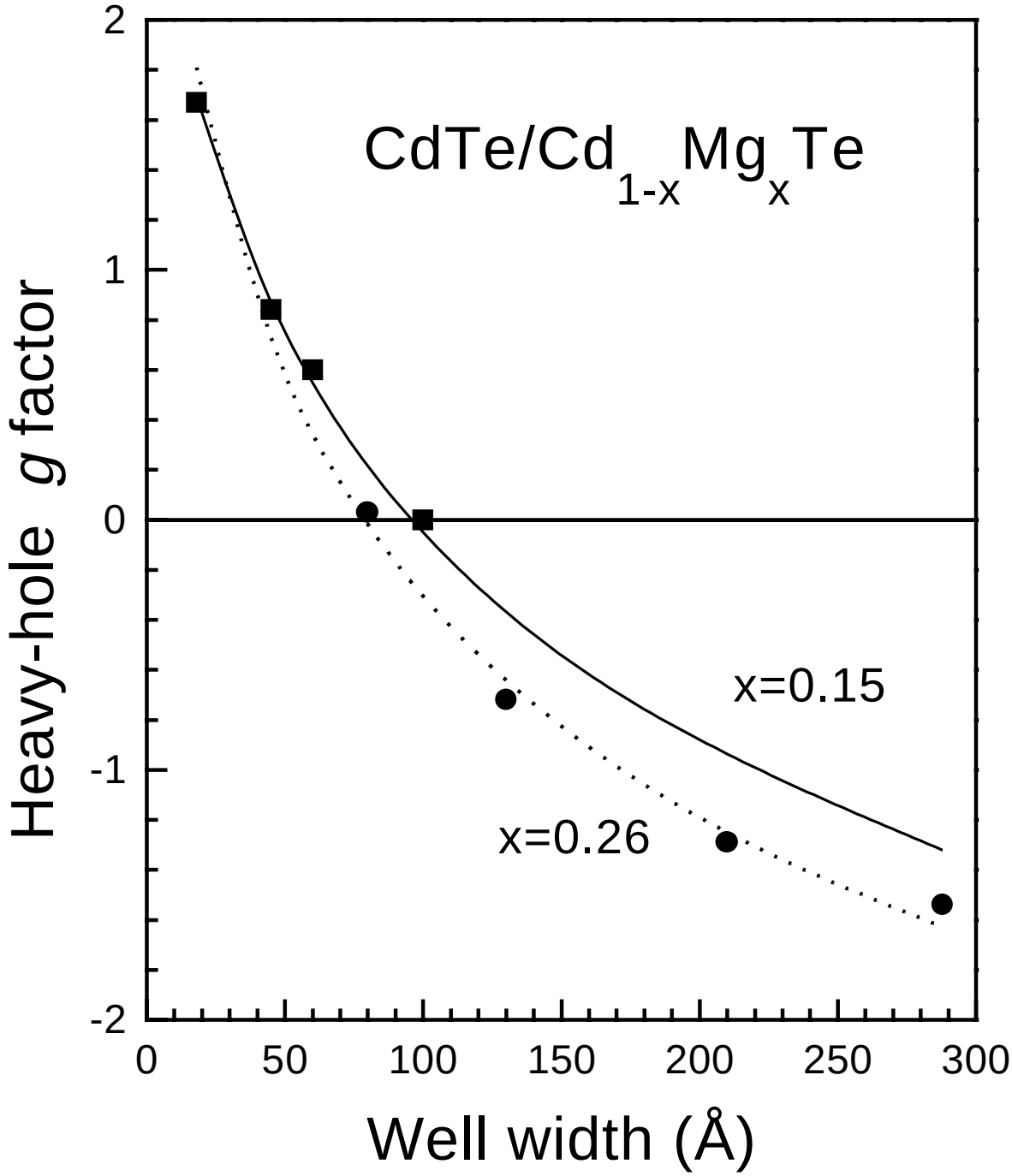

Fig. 2. Kiselev et al., A2B6 Conference in Grenoble